RAA 2015 Vol. **15** No. **10**, 1751–1757 doi: 10.1088/1674–4527/15/10/012
http://www.raa-journal.org *http://www.iop.org/journals/raa*

***R**esearch in*
***A**stronomy and*
***A**strophysics*

Spacecraft Doppler tracking with possible violations of LLI and LPI: upper bounds from one-way measurements on MEX

Yi Xie[1,2,3] and Yong Huang[4]

[1] School of Astronomy and Space Science, Nanjing University, Nanjing 210093, China; *yixie@nju.edu.cn*
[2] Shanghai Key Laboratory of Space Navigation and Position Techniques, Shanghai 200030, China
[3] Key Laboratory of Modern Astronomy and Astrophysics, Nanjing University, Ministry of Education, Nanjing 210093, China
[4] Shanghai Astronomical Observatory, Chinese Academy of Sciences, Shanghai 200030, China

Received 2014 June 29; accepted 2015 March 13

Abstract We analyze the post-fit residuals of one-way Doppler tracking data from the Mars Express (MEX) spacecraft to test possible violations of local Lorentz invariance (LLI) and local position invariance (LPI). These one-way Doppler observations were carried out on 2011 August 7 for about 20 minutes at Sheshan Station of Shanghai Astronomical Observatory in China. These downlink signals were sent by MEX for telemetry at X-band. Because we are not able to decode the data in the form of telemetry and separate them from the carrier frequency, this makes the post-fit residuals of the Doppler data degrade to the level of 0.1 m s^{-1}. Even so, the residuals can still impose upper bounds on LLI and LPI at 10^{-1}, which is consistent with the prediction based on our analysis of the detectability. Although the upper bounds given by three-way Doppler tracking of MEX are better than those obtained in the present work, one-way Doppler measurements still provide a unique chance to test possible violations of LLI and LPI far from the ground stations.

Key words: space vehicles — techniques: radial velocities — gravitation

1 INTRODUCTION

Spacecraft Doppler tracking is a successful technique for control and navigation in deep space missions (Kruger 1965; Moyer 2005). This technique can also be implemented for scientific research, such as fundamental physics (e.g. Chapter 7.8 of Kopeikin et al. 2011). In the present work, we will try to test the Einstein equivalence principle (EEP) by using one-way Doppler tracking.

EEP is essential for constructing general relativity (GR) and all other metric theories of gravity. It depends on the weak equivalence principle, local Lorentz invariance (LLI), and local position invariance (LPI) (see Will 1993, 2006; Kopeikin et al. 2011, for more details). LLI and LPI can be tested by measuring the redshift of the frequency of a signal when its emitter moves in a gravitational field (e.g. Krisher 1990). EEP has been confirmed at levels from $\sim 10^{-4}$ to $\sim 10^{-2}$ by experiments in the vicinity of the Earth (Vessot et al. 1980) and in interplanetary space (e.g. Krisher et al. 1990, 1993).

All of these experiments relied on a one-way radio signal transmitted from the spacecraft to ground stations. The transmitted frequency was based on an onboard frequency standard. However, such an onboard standard is much less stable than ground-based standards and is limited by its own noise. One solution for this is to use two-way or three-way Doppler tracking. Considering these advantages, Deng & Xie (2014) extended the relativistic theories of two-way and three-way Doppler tracking by including possible violations of LLI and LPI. With this model, Zhang et al. (2014) analyzed the post-fit residuals of three-way Doppler tracking data from Mars Express (MEX) for determining bounds on LLI and LPI. These Doppler observations were carried out from 2009 August 7 to 8, with an uplink station administered by the European Space Agency (ESA) at New Norcia in Australia and three downlink stations at Shanghai, Kunming and Urumqi in China. It was found by Zhang et al. (2014) that these observations impose preliminary bounds on LLI at the level of 10^{-2}, but they are not suitable for testing LPI because of the configuration of these stations and the insufficient accuracy of the observations.

In the present work, as a demonstration of the capabilities of the Chinese deep space tracking system and software used for data processing, we will try to test EEP by utilizing one-way Doppler tracking data from MEX. Although this kind of measurement suffers various types of noise, it still provides us with unique access to the possible violations of EEP which might be far from ground stations and associated with the spacecraft in deep space. By contrast, three-way Doppler tracking is only sensitive to the possible violations of EEP associated with two ground stations and these violations cannot affect two-way Doppler tracking under a linear approximation of the light time solution (Deng & Xie 2014). One-way measurements on MEX were conducted by the Shanghai Astronomical Observatory (SHAO) in China on 2011 August 7 for about 20 minutes. The downlink signals were sent by MEX in the form of telemetry. Because we are not able to decode the data contained in telemetry and separate them from the carrier frequency, we have to treat them as unmodeled or mismodeled components in the post-fit residuals. These residuals will be used to obtain upper bounds on LLI and LPI.

The rest of the paper is organized as follows. Section 2 is devoted to describing the model of one-way Doppler tracking with possible violations of LLI and LPI. Their detectability will also be analyzed and some prediction will be made. In Section 3, we present the one-way Doppler observations of MEX and their data reduction. The post-fit residuals are taken to estimate the upper bounds on LLI in Section 4. Finally, in Section 5, we summarize our results.

2 MODEL OF ONE-WAY DOPPLER TRACKING WITH VIOLATIONS OF LLI AND LPI

In order to test EEP, we adopt the parametrized model of one-way Doppler tracking according to Krisher et al. (1993). After applying the linear approximation of the light time solution (see Chapter 8 in Moyer 2005, for details), we have the deviation of the redshift δz from the prediction by EEP, which is

$$\delta z = \delta z_{\mathrm{LLI}} + \delta z_{\mathrm{LPI}} + \mathcal{O}(\epsilon^3)\,, \tag{1}$$

where δz_{LLI} and δz_{LPI} are respectively caused by the possible violations of LLI and LPI, which are

$$\delta z_{\mathrm{LLI}} \;=\; \frac{1}{2}\epsilon^2\bar{\beta}_{\mathrm{R}}\boldsymbol{v}_{\mathrm{R}}^2(t_{\mathrm{R}}) - \frac{1}{2}\epsilon^2\bar{\beta}_{\mathrm{E}}\boldsymbol{v}_{\mathrm{E}}^2(t_{\mathrm{R}})\,, \tag{2}$$

$$\delta z_{\mathrm{LPI}} \;=\; \epsilon^2\sum_A \bar{\alpha}_{\mathrm{R}}^A U_A[\boldsymbol{y}_{\mathrm{R}}(t_{\mathrm{R}})] - \epsilon^2\sum_A \bar{\alpha}_{\mathrm{E}}^A U_A[\boldsymbol{y}_{\mathrm{E}}(t_{\mathrm{R}})]\,. \tag{3}$$

In this case $\epsilon \equiv c^{-1}$ and c is the speed of light. Here, $\boldsymbol{y}_{\mathrm{E}}$ and $\boldsymbol{y}_{\mathrm{R}}$ are respectively the positional vectors of the emitter and the receiver in the Barycentric Celestial Reference System (BCRS) (Soffel et al. 2003), and $\boldsymbol{v}_{\mathrm{E}}$ and $\boldsymbol{v}_{\mathrm{R}}$ are their velocities. Possible violations of LLI can be tested by fitting the dimensionless parameters $\bar{\beta}_{\mathrm{R}}$ and $\bar{\beta}_{\mathrm{E}}$, which are respectively associated with the receiver and the emitter. If LLI holds true, then $\bar{\beta}_{\rm R/E}=0$. Possible violations of LPI can be tested by fitting the dimensionless parameters $\bar{\alpha}^A_{\rm R}$ and $\bar{\alpha}^A_{\rm E}$, which are respectively associated with the receiver and the emitter in the gravitational field of body A. If there is no violation of LPI, then $\bar{\alpha}^A_{\rm R/E}=0$.

Before applying this model to one-way Doppler observations, it is first necessary for us to investigate the detectability of these parameters. It is worth mentioning that this discussion of detectability is *not* a statistical estimation of the parameters. They will be statistically estimated by the method of weighted least squares in Section 4. Considering a spacecraft around Mars and a ground station on the Earth, we can rewrite $\delta z_{\rm LLI}$ (see Eq. (2)) as

$$\delta z_{\rm LLI}=\frac{1}{2}\epsilon^2\left[\bar{\beta}_{\rm R}(\boldsymbol{v}_\oplus+\boldsymbol{V}_{\rm S})^2-\bar{\beta}_{\rm E}(\boldsymbol{v}_{\rm Mars}+\boldsymbol{V}_{\rm P})^2\right], \tag{4}$$

where $\boldsymbol{v}_\oplus$ and $\boldsymbol{v}_{\rm Mars}$ are respectively the velocities of the Earth and Mars in the BCRS; $\boldsymbol{V}_{\rm S}$ is the local velocity of the station in the Geocentric Celestial Reference System (GCRS) (Soffel et al. 2003); and $\boldsymbol{V}_{\rm P}$ is the local velocity of the spacecraft with respect to the center of mass of Mars. If we assume $\bar{\beta}_{\rm S_1}=\bar{\beta}_{\rm S_2}=\bar{\beta}$, $v_\oplus\gg V_{\rm S}$ and $v_{\rm Mars}\gg V_{\rm P}$, then $\delta z_{\rm LLI}$ can be simplified as

$$\delta z_{\rm LLI}=\frac{1}{2}\epsilon^2\bar{\beta}(\boldsymbol{v}^2_\oplus-\boldsymbol{v}^2_{\rm Mars})\,. \tag{5}$$

Because $v_\oplus\sim3.0\times10^4$ m s^{-1} and $v_{\rm Mars}\sim2.4\times10^4$ m s^{-1}, we can obtain

$$\bar{\beta}\sim2c^2\delta z_{\rm LLI}(\boldsymbol{v}^2_\oplus-\boldsymbol{v}^2_{\rm Mars})^{-1}\sim0.5\times\left(\frac{\delta z_{\rm LLI}}{10^{-9}}\right). \tag{6}$$

This means if the residuals of one-way Doppler observation are at the level of 10^{-9}, then the parameter $\bar{\beta}$ can be determined to the level of $\sim10^{-1}$ when the violation of LPI is neglected. The causes of the residuals might come from several sources, such as various types of noise, which might be unmodeled and/or mismodeled in the software, and some specific signals which cannot be decoded and separated from the carrier frequency by the observer. Although this rough estimation is independent of the local velocities of the station and spacecraft, it can give the leading order of the detectability. For a realistic data analysis, these two local velocities must be included in the model, as we will do in Section 4.

For the detectability of violations of LPI, if only the monopole component of the gravitational field of the Sun is taken into account, then we can rewrite $\delta z_{\rm LPI}$ (see Eq. (3)) as

$$\delta z_{\rm LPI}=\epsilon^2\left[\bar{\alpha}^\odot_{\rm R}\frac{GM_\odot}{|\boldsymbol{y}_\odot-\boldsymbol{y}_\oplus-\boldsymbol{Y}_{\rm S}|}-\bar{\alpha}^\odot_{\rm E}\frac{GM_\odot}{|\boldsymbol{y}_\odot-\boldsymbol{y}_{\rm Mars}-\boldsymbol{Y}_{\rm P}|}\right], \tag{7}$$

where $\boldsymbol{y}_\odot$, $\boldsymbol{y}_\oplus$ and $\boldsymbol{y}_{\rm Mars}$ are respectively the positions of the Sun, Earth and Mars in the BCRS; $\boldsymbol{Y}_{\rm S}$ is the local position of the station in the GCRS; and $\boldsymbol{Y}_{\rm P}$ is the local position of the spacecraft with respect to the center of mass of Mars. If we assume $\bar{\alpha}^\odot_{\rm S_1}\sim\bar{\alpha}^\odot_{\rm S_2}=\bar{\alpha}^\odot$ and make use of the conditions that $|\boldsymbol{y}_\odot-\boldsymbol{y}_\oplus|\gg|\boldsymbol{Y}_{\rm S}|$ and $|\boldsymbol{y}_\odot-\boldsymbol{y}_{\rm Mars}|\gg|\boldsymbol{Y}_{\rm P}|$, then $\delta z_{\rm LPI}$ can be simplified as

$$\delta z_{\rm LPI}=\epsilon^2\bar{\alpha}^\odot\left(\frac{GM_\odot}{|\boldsymbol{y}_\odot-\boldsymbol{y}_\oplus|}-\frac{GM_\odot}{|\boldsymbol{y}_\odot-\boldsymbol{y}_{\rm Mars}|}\right). \tag{8}$$

Since $|\boldsymbol{y}_\odot-\boldsymbol{y}_\oplus|\sim1$ au and $|\boldsymbol{y}_\odot-\boldsymbol{y}_{\rm Mars}|\sim1.5$ au, we can estimate that

$$\bar{\alpha}^\odot\sim c^2\delta z_{\rm LPI}\left(\frac{GM_\odot}{|\boldsymbol{y}_\odot-\boldsymbol{y}_\oplus|}-\frac{GM_\odot}{|\boldsymbol{y}_\odot-\boldsymbol{y}_{\rm Mars}|}\right)^{-1}\sim0.3\times\frac{\delta z_{\rm LPI}}{10^{-9}}\,. \tag{9}$$

This means that when the residuals of the one-way Doppler data are at the level of 10^{-9}, the parameter $\bar{\alpha}^\odot$ can be determined to $\sim10^{-1}$ when the violation of LLI is neglected. Thus, Equations (6) and

(9) roughly describe the detectability of a possible violation of LLI and LPI by the one-way Doppler tracking. It is worth mentioning again that these two equations are just crude estimations: they might be able to show leading effects but the full model (see Eqs. (1)–(3)) must be used in realistic data analyses.

In the following parts of this work, we will analyze the post-fit residuals of the one-way Doppler tracking data of MEX (see Sect. 3) and use these residuals to estimate the upper bounds on these violations according to Equations (1)–(3) (see Sect. 4).

3 ONE-WAY DOPPLER TRACKING OF MEX

In the observational study, we acquired the downlink signals from MEX at the X-band (8.4 GHz), which started at 04:18 on 2011 August 7 (UTC) and ended at 04:41 on the same day (UTC). These signals did not match any known radio science campaigns associated with MEX[1] and they were sent in the form of telemetry (Pätzold 2014, private communication). The carrier frequency of the telemetry signals was generated by the onboard frequency system, which was an ultra-stable oscillator (Pätzold et al. 2004). The downlink signals were received by a 25-meter dish at the Sheshan Station of SHAO. The frequency standard used by the Sheshan Station was an H-maser with a stability of about 10^{-15} in a day (Zheng et al. 2013), and we also acquired our VLBI observations at this station. It is worth mentioning that we were not able to decode the data in the form of telemetry and separate them from the carrier frequency, so we had to treat them as unmodeled and/or mismodeled components in the data processing. The duration of the observation was 23 minutes and 275 data points were obtained. These one-way observation data were processed by the software MARSODP (Huang et al. 2009) to *simultaneously* determine the orbit of MEX and the frequency of the downlink which was previously unknown. MARSODP was developed by a group from SHAO. It can reduce data from two/three-way ranging, one/two/three-way Doppler tracking, VLBI and other types of observations. However, a better way to perform such a test, as was done with the experiment using the Galileo spacecraft (Krisher et al. 1993), is to determine the position and velocity of the spacecraft *independently* from two/three-way Doppler tracking and the range measurements which are referenced to the frequency standards of the ground stations.

As a demonstration on the capabilities of the Chinese deep space tracking system and software used for data processing, we use the post-fit residuals of the one-way Doppler tracking to estimate the upper bounds on possible violations of LLI and LPI. These residuals were obtained by fitting the observational data with the standard model which is built on Newton's law and Einstein's GR (see Huang et al. 2009, for details). Therefore, the effects of violations of LLI and LPI were not modeled in MARSODP and the parameters $\bar{\beta}_{\mathrm{R/E}}$ and $\bar{\alpha}^{A}_{\mathrm{R/E}}$ were not determined in the fitting. In this sense, the results that we obtain in the next section may not be considered to be genuine "constraints" (they would be so if one solved for them in a covariance analysis by reanalyzing the data with modified software that includes these effects), but they are preliminary indications of acceptable upper limits computed by the best contemporary knowledge (see Iorio 2014, for a further discussion).

Figure 1 shows the post-fit residuals δv (left panel) and their statistical histograms (right panel) after MARSODP was used to process the one-way Doppler tracking data that were obtained by SHAO. The origin of the time coordinates is chosen to coincide with $04^{\mathrm{h}}18^{\mathrm{m}}10.5^{\mathrm{s}}$ on 2011 August 7 (UTC). The mean value of these residuals $\langle\delta v\rangle$ is -2.5×10^{-4} m s^{-1} and the standard deviation $\sigma_{\delta v}$ is about 0.1 m s^{-1}. It is worth mentioning that $\sigma_{\delta v}$ is much larger than the observational errors at SHAO. The Doppler frequency noise of SHAO's hardware is at the level of $\sim$mHz in S and X bands, corresponding to the level of $\sim 10^{-4}$ m s^{-1} in radial velocity (Cao et al. 2010; Zheng et al. 2013), which is comparable with ESA's error budget for MEX (Pätzold et al. 2004). For comparison, by making use of MARSODP, the mean value of the post-fit residuals, derived from three-way Doppler tracking of MEX that was carried out in 2009 by SHAO, was $\sim 10^{-4}$ m s^{-1} and the

[1] The Geosciences Node of NASA's Planetary Data System (PDS) archives: *http://pds-geosciences.wustl.edu/*.

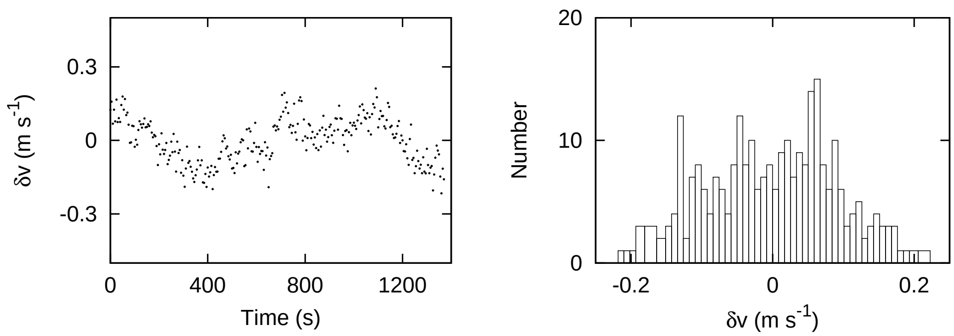

Fig. 1 The post-fit residuals δv (*left panel*) and their statistical histograms (*right panel*) after MARSODP was used to process the one-way Doppler tracking data obtained by SHAO in China. The origin of the time coordinates is chosen to coincide with $04^{\rm h}18^{\rm m}10.5^{\rm s}$ on 2011 August 7 (UTC).

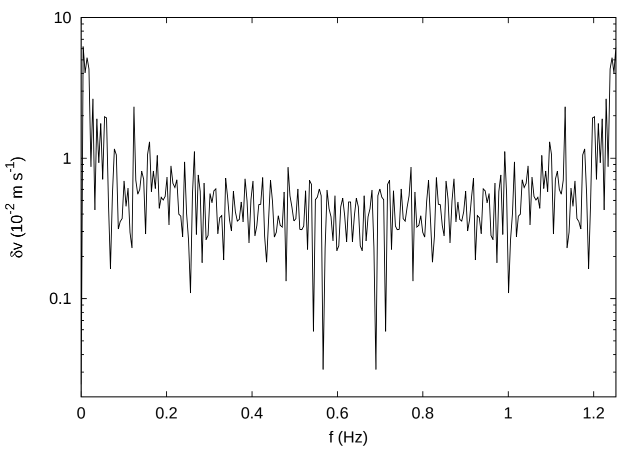

Fig. 2 The spectrum of residuals δv (see the left panel of Fig. 1). There are 21 peaks with amplitudes larger than 10^{-2} m s^{-1}, which contribute a lot of the fluctuations in δv. The highest peak has a frequency of 4.57 mHz and an amplitude of 6.22×10^{-2} m s^{-1}.

standard deviation of these residuals was about 3×10^{-4} m s^{-1}. These values were consistent with the observational errors of $\sim 10^{-4}$ m s^{-1} (see Cao et al. 2010; Cao et al. 2011, for details).

We think that a much larger $\sigma_{\delta v}$ might be caused by the telemetry data embedded in the carrier frequency. Because we are not able to decode and separate them, MARSODP treats them as "signals" of the carrier frequency, regardless if they are unmodeled and/or mismodeled components.

Figure 2 shows the spectrum of the post-fit residuals δv in the frequency domain. The range of the frequency domain is determined by our sampling interval of 5 s. The resolution of the frequencies is limited due to the short time span of the observation. There are 21 peaks that have amplitudes larger than 10^{-2} m s^{-1}, which contribute a lot to the the fluctuations in δv (see left panel of Fig. 1). The highest peak has a frequency of 4.57 mHz and an amplitude of 6.22×10^{-2} m s^{-1}. Although the residuals returned from MARSODP are dominated by the telemetry signals, they can still provide some information and can be used to obtain the upper bounds on LLI and LPI, as our analysis on the detectability described in the previous section indicates.

4 UPPER BOUNDS ON LLI

We will estimate the upper bounds on violations of LLI and LPI by using the method of minimizing the weighted sum of squares, called weighted least squares

$$S = \sum_i w_i (\epsilon \delta v_i - \delta z_i)^2 , \tag{10}$$

where δv_i and δz_i are respectively the post-fit residual and the theoretical prediction by Equation (1) for the ith data point. The factor w_i is the statistical weight for the ith data point. It is quite common that w_i takes the value of σ_i^{-2}, where σ_i is the observational error for the ith point, such as in the case of Zhang et al. (2014). However, as was shown in Section 3, the post-fit residuals are much larger than the observational errors in our one-way Doppler measurements so that the observational errors are not a suitable choice for weights. Instead, we *set* $w_i = \Delta v_i^{-2}$, where Δv_i is the deviation of the average for δv_i, i.e. $\Delta v_i = \delta v_i - \langle \delta v \rangle$.

Our estimation will be divided into three further cases. In Case I, we *assume* that $\bar{\beta}_{\rm R}$ and $\bar{\beta}_{\rm E}$ are the *free* parameters and make the other parameters vanish. It is found that, in Case I, $\bar{\beta}_{\rm R} = (0.56 \pm 1.04) \times 10^{-1}$ and $\bar{\beta}_{\rm E} = (0.76 \pm 1.42) \times 10^{-1}$. In Case II, we *assume* that $\bar{\beta}_{\rm R} = \bar{\alpha}^{\odot}_{\rm R} = \bar{\beta}'_{\rm R}$ and $\bar{\beta}_{\rm E} = \bar{\alpha}^{\odot}_{\rm E} = \bar{\beta}'_{\rm E}$, which means the Sun's contribution to Equation (3) will be taken into account, and we set the other parameters to zero. We find that $\bar{\beta}'_{\rm R} = (0.53 \pm 0.98) \times 10^{-1}$ and $\bar{\beta}'_{\rm E} = (0.76 \pm 1.42) \times 10^{-1}$ in Case II. In Case III, we *assume* that $\bar{\beta}_{\rm R} = \bar{\beta}_{\rm E} = \bar{\beta}$ and $\bar{\alpha}^{\odot}_{\rm R} = \bar{\alpha}^{\odot}_{\rm E} = \bar{\alpha}^{\odot}$ and we find $\bar{\beta} = (0.74 \pm 1.39) \times 10^{-1}$ and $\bar{\alpha}^{\odot} = (-0.29 \pm 0.54) \times 10^{-1}$. The results of these cases are summarized in Table 1 and they are found to be consistent with our analysis on the detectability of the parameters in Equations (6) and (9).

Table 1 Summary of Preliminary Bounds on LLI and LPI

Case	$\bar{\beta}_{\rm R}$ (10^{-1})	$\bar{\beta}_{\rm E}$ (10^{-1})	$\bar{\alpha}^{\odot}_{\rm R}$ (10^{-1})	$\bar{\alpha}^{\odot}_{\rm E}$ (10^{-1})	Assumption
I	0.56 ± 1.04	0.76 ± 1.42	–	–	$\bar{\alpha}^{\odot}_{\rm R} = \bar{\alpha}^{\odot}_{\rm E} = 0$
II	0.53 ± 0.98	0.76 ± 1.42	$= \bar{\beta}_{\rm R}$	$= \bar{\beta}_{\rm E}$	$\bar{\beta}_{\rm R} = \bar{\alpha}^{\odot}_{\rm R}$, $\bar{\beta}_{\rm E} = \bar{\alpha}^{\odot}_{\rm E}$
III	0.74 ± 1.39	$= \bar{\beta}_{\rm R}$	-0.29 ± 0.54	$= \bar{\alpha}^{\odot}_{\rm R}$	$\bar{\beta}_{\rm R} = \bar{\beta}_{\rm E}$, $\bar{\alpha}^{\odot}_{\rm R} = \bar{\alpha}^{\odot}_{\rm E}$

We also find that, since the Earth and Mars are barely moving in the BCRS during the short duration of our tracking (about 20 minutes), other combinations of parameters for estimation are inappropriate and will give unphysical bounds. Although the upper bounds given by three-way Doppler tracking (Zhang et al. 2014) are better than those obtained in the present work by about a factor of 10, one-way Doppler measurements still impose a unique chance to test possible violations of EEP far from the ground tracking stations.

5 CONCLUSIONS

We analyze the post-fit residuals associated with one-way Doppler tracking of MEX. These Doppler observations were carried out from 2011 August 7, with the Sheshan Station of SHAO in China. The downlink signals were sent by MEX at X-band in the form of telemetry. We find that, because we are not able to decode the data in the form of telemetry and isolate them from the carrier frequency, this makes the post-fit residuals of the one-way data degrade to the level of 0.1 m s^{-1}. However, they can still impose upper bounds on LLI and LPI at 10^{-1}, which are consistent with the prediction based on our analysis of the detectability.

Meanwhile, this investigation is rather limited by the short duration of the tracking and lack of three-way Doppler tracking for independent orbit determination of MEX. These two factors are helpful to solidly and robustly pin down and separate different noises in the one-way measurements.

Therefore, we suggest that a specific carrier frequency for one-way Doppler tracking, an independent method of orbit determination and a long time span for observations are indispensable ingredients for Chinese future deep space missions, which will aim to effectively test EEP.

Acknowledgements We would like to express our appreciation to Prof. M. Pätzold for the extremely helpful advice on this work. This work is funded by the National Natural Science Foundation of China (Grant Nos. 11103010, 11573015 and 11073047), the Fundamental Research Program of Jiangsu Province of China under No. BK2011553, the Research Fund for the Doctoral Program of Higher Education of China (No. 20110091120003), the Fundamental Research Funds for the Central Universities (Grant No. 20620140586) and the Opening Project of Shanghai Key Laboratory of Space Navigation and Position Techniques (Grant No. 14DZ2276100).

References

Cao, J.-F., Huang, Y., Hu, X.-G., & Hu, S. J. 2011, Journal of Astronautics (in Chinese), 32, 1583

Cao, J., Huang, Y., Hu, X., Ma, M., & Zheng, W. 2010, Chinese Science Bulletin, 55, 3654

Deng, X.-M., & Xie, Y. 2014, RAA (Research in Astronomy and Astrophysics), 14, 319

Huang, Y., Hu, X.-G., Cao, J.-F., & Li, P. J. 2009, Journal of Spacecraft TT& C Technology (in Chinese), 28, 83

Iorio, L. 2014, International Journal of Modern Physics D, 23, 50006

Kopeikin, S., Efroimsky, M., & Kaplan, G. 2011, Relativistic Celestial Mechanics of the Solar System (Berlin: Wiley-VCH)

Krisher, T. P. 1990, Modern Physics Letters A, 5, 1809

Krisher, T. P., Anderson, J. D., & Campbell, J. K. 1990, Physical Review Letters, 64, 1322

Krisher, T. P., Morabito, D. D., & Anderson, J. D. 1993, Physical Review Letters, 70, 2213

Kruger, B. 1965, A Critical Review of the Use of Doppler Frequency for Range and Range Rate Measurements, in GSFC Document X-507-65-386 and NASA TM X-55416 (*http://ntrs.nasa.gov/archive/nasa/casi.ntrs.nasa.gov/19660010160.pdf*)

Moyer, T. D. 2005, Formulation for Observed and Computed Values of Deep Space Network Data Types for Navigation, 3 (NYSE: John Wiley & Sons)

Pätzold, M., Neubauer, F. M., Carone, L., et al. 2004, in ESA Special Publication, 1240, Mars Express: the Scientific Payload, ed. A. Wilson & A. Chicarro, 141

Soffel, M., Klioner, S. A., Petit, G., et al. 2003, AJ, 126, 2687

Vessot, R. F. C., Levine, M. W., Mattison, E. M., et al. 1980, Physical Review Letters, 45, 2081

Will, C. M. 1993, Theory and Experiment in Gravitational Physics (Cambridge: Cambridge Univ. Press)

Will, C. M. 2006, Living Reviews in Relativity, 9, 3

Zhang, Y.-F., Zhang, X.-Z., Liu, J.-H., Huang, Y., & Xie, Y. 2014, RAA (Research in Astronomy and Astrophysics), 14, 1201

Zheng, W.-M., Ma, M.-L., & Wang, W.-B. 2013, Journal of Astronautics (in Chinese), 34, 1462